

## Ominelite, (Fe,Mg)Al<sub>3</sub>BSiO<sub>9</sub> (Fe<sup>2+</sup> analogue of grandidierite), a new mineral from porphyritic granite in Japan

YOSHIKUNI HIROI,<sup>1,\*</sup> EDWARD S. GREW,<sup>2</sup> YOICHI MOTOYOSHI,<sup>3</sup> DONALD R. PEACOR,<sup>4</sup> ROLAND C. ROUSE,<sup>4</sup> SATOSHI MATSUBARA,<sup>5</sup> KAZUMI YOKOYAMA,<sup>5</sup> RITSURO MIYAWAKI,<sup>5</sup> JAMES J. MCGEE,<sup>6</sup> SHU-CHUN SU,<sup>7</sup> TOMOKAZU HOKADA,<sup>3</sup> NOBORU FURUKAWA,<sup>1</sup> AND HIROSHI SHIBASAKI<sup>8</sup>

<sup>1</sup>Department of Earth Sciences, Chiba University, Yayoicho, Inage-ku, Chiba 263-8522, Japan

<sup>2</sup>Department of Geological Sciences, University of Maine, Orono, Maine 04469, U.S.A.

<sup>3</sup>Department of Crustal Studies, National Institute of Polar Research, Kaga, Itabashi-ku, Tokyo 173-8515, Japan

<sup>4</sup>Department of Geological Sciences, University of Michigan, Ann Arbor, Michigan 48109, U.S.A.

<sup>5</sup>Department of Geology, National Science Museum, Hyakunincho, Shinjuku-ku, Tokyo 169-0073, Japan

<sup>6</sup>Department of Geological Sciences, University of South Carolina, Columbia, South Carolina 29208, U.S.A.

<sup>7</sup>Hercules Research Center, 500 Hercules Road, Wilmington, Delaware 19808, U.S.A.

<sup>8</sup>Overseas Activities Department, Metal Mining Agency of Japan, Toranomon, Minato-ku, Tokyo 105-0001, Japan

### ABSTRACT

Ominelite, (Fe,Mg)Al<sub>3</sub>BSiO<sub>9</sub>, is the Fe<sup>2+</sup> analog of grandidierite. The mineral occurs as elongated and euhedral to equant and anhedral grains in close association with sekaninaite (Fe-dominant analogue of cordierite), garnet, biotite, andalusite, topaz, alkali feldspar, plagioclase, muscovite, quartz, dumortierite, schorl, zircon, ilmenite, apatite, monazite, and pyrite in a porphyritic granite of Miocene age exposed along the Misen River in Tenkawa, Yoshino, Nara Prefecture, Japan (34°12'40"N, 135°53'40"E). Temperatures <700 °C and pressures below 4 kbars are suggested for the formation of ominelite and associated sekaninaite, topaz, andalusite and dumortierite. The Al-rich minerals could be either magmatic or restitic in origin. A representative electron microprobe analysis of ominelite is SiO<sub>2</sub> 19.34, TiO<sub>2</sub> <0.01, Al<sub>2</sub>O<sub>3</sub> 48.85, FeO 19.37, MnO 0.43, MgO 1.33, CaO <0.01, P<sub>2</sub>O<sub>5</sub> 0.13, B<sub>2</sub>O<sub>3</sub> 10.91 wt%, total 100.36 wt%, corresponding to Fe<sub>0.85</sub>Mg<sub>0.10</sub>Mn<sub>0.02</sub>Al<sub>3.01</sub>B<sub>0.99</sub>P<sub>0.01</sub>Si<sub>1.01</sub>O<sub>9</sub>. Mohs' hardness is about 7. No cleavage is observed. Its color is blue, and the streak is pale blue. It is pleochroic  $X = Z =$  pale blue-green and  $Y =$  colorless. Optically, it is biaxial (–) and, at  $\lambda = 589$  nm, has  $\alpha = 1.631$  (1),  $\beta = 1.654$  (1),  $\gamma = 1.656$  (1),  $2V_x$  (meas.) = 31.5 (6)°.  $Y = c$  (prism elongation direction). Dispersion is  $v \gg r$ . Major lines in the powder pattern [ $d$  in Å, ( $hkl$ )] are 5.57(m)(020), 5.21(vs)(200), 3.73(m)(121), 3.51(m)(130), 2.97(s)(101), 2.79(s)(040), 2.18(s)(150, 421, 312). Space group is *Pbnm*. Lattice parameters are  $a = 10.343$  (2),  $b = 11.095$  (1),  $c = 5.7601$  (8) Å and  $V = 661.0(2)$  Å<sup>3</sup>,  $Z = 4$ ,  $D_{\text{calc}} = 3.169$  g/cm<sup>3</sup>. Refinement of the structure confirms that ominelite is isostructural with grandidierite with no detectable substitution of Al by Fe<sup>3+</sup>.

### INTRODUCTION

Since its discovery some 100 years ago at Andrahomana, Madagascar (Lacroix 1902), grandidierite, (Mg,Fe)Al<sub>3</sub>BSiO<sub>9</sub>, has been described from about 40 localities worldwide in regionally and contact metamorphosed pelitic and calcareous rocks, migmatites, and granulite-facies pegmatite (e.g., Grew 1996; Grew et al. 1998). McKie (1965) was the first to determine the presently accepted formula, which was confirmed by Stephenson and Moore's (1968) crystal structure refinement. The first analyses carried out by Pisani (Lacroix 1903) and Raoult (Lacroix and de Gramont 1919) on material from the type locality in Madagascar gave Mg > total Fe, but the reported presence of CaO, alkalis and water implies that the analyzed material must not have been pure. Subsequent analyses of samples from the type locality gave Mg > Fe<sup>2+</sup>, i.e.,  $X_{\text{Fe}} =$

$\text{Fe}^{2+}/(\text{Fe}^{2+} + \text{Mg}) = 0.45\text{--}0.49$  (Grew et al. 1998) as do most analyses of material from other localities (e.g., Herd et al. 1984; Grew 1996), including McKie's (1965) magnesian sample from Sakatelo, Madagascar. Consequently, grandidierite is generally considered to be the Mg-dominant end-member (e.g., Mandarino 1999). Compositions with Fe<sup>2+</sup> > Mg have been reported from Almgjotheii, Norway ( $X_{\text{Fe}} = 0.50\text{--}0.81$ , Huijsmans et al. 1982; Grew et al. 1998), Morton Pass, Wyoming (0.58, Grant and Frost 1990), possibly Bellerberg, Eifel, Germany (~0.5, Blass and Graf 1994), and Mt. Stafford, Australia (0.50–0.55, calculated from Greenfield et al. 1998). However, this Fe<sup>2+</sup>-dominant material was sparse, fine-grained and not well suited for describing Fe-dominant grandidierite as a distinct species.

Andalusite-sekaninaite-biotite porphyritic granite cropping out in the Misen pluton, Omine Mountains, Nara Prefecture, Japan, is noteworthy for extreme enrichment of Fe<sup>2+</sup> relative to Mg and in containing the borosilicate minerals dumortierite,

\* E-mail: yhiroi@earth.s.chiba-u.ac.jp

schorl, and Fe-dominant grandierite in which  $X_{Fe}$  exceeds 0.9 in some specimens. The last proved to be suitable for characterizing Fe<sup>2+</sup>-dominant grandierite as the new mineral ominelite, which is named for the Omine Mountains. The new mineral and name have been approved by the Commission on New Minerals and Mineral Names of the IMA. Type material is deposited in the Department of Geology, National Science Museum, Tokyo, and at the Department of Earth Sciences, Chiba University, Chiba, Japan.

Occurrence of ominelite in porphyritic granite is a new paragenesis for the grandierite-ominelite solid solution series, and a relatively low-temperature one. In the present paper we not only describe ominelite as a new mineral and report its crystal structure, but also compare it to grandierite and consider its formation in a magmatic setting.

### OCCURRENCE

The Omine acid rocks are among the Middle Miocene granitoids intruding the Cretaceous-Paleogene accretionary complexes of the Shimanto Belt in the Outer Zone between the Median Tectonic Line and the Pacific coast of Southwest Japan (Fig. 1). The isotopic ages of these granitoids range from 14 Ma to 17 Ma (Shibata 1978; Hasebe et al. 2000), essentially contemporaneous with the climax of the back-arc opening of the Sea of Japan (e.g., Takahashi 1986; Terakado et al. 1988). Petrographic characteristics indicate that both I- and S-type intrusions (Chappell and White 1974) are present in the Outer Zone. The I-type rocks contain hornblende and occur in the northern part of the zone, whereas the S-type rocks characteristically carry cordierite and biotite with or without andalusite, sillimanite, muscovite, garnet, and orthopyroxene, and are distributed on the Pacific side (e.g., Kawasaki 1980a, 1980b; Takahashi et al. 1980; Murata 1982, 1984; Murata et al. 1983;

Murata and Itaya 1987). The boundary between the two groups runs nearly parallel to the Nankai Trough, the deepest part of the Shikoku basin (Fig. 1). The Middle Miocene Outer Zone granitoids may be related to subduction of the young and hot Shikoku basin, but they could also have formed when a hot region caused by mantle convection moving northwest from the Shikoku basin to the Japan Sea (Terakado et al. 1988).

The Omine acid rocks were intruded as small bodies over a distance of about 45 km in the N-S direction in the central Kii Peninsula (Fig. 1). The northernmost pluton and associated small satellite intrusives consist of I-type tonalitic granodiorite, whereas bodies to the south consist of S-type granite to granodiorite (e.g., Murata 1984; Murata and Yoshida 1985; Shiida et al. 1989). Rocks containing the most iron-rich ominelite occur in one of the northernmost S-type intrusives, which crop out along the Misen River. This small (1.3 × 0.3 km) Misen (or Shirakawa-hatcho) pluton is fine- to medium-grained, massive porphyritic granite and granodiorite and had only a weak thermal effect on the sedimentary country rocks. Ominelite less enriched in Fe is found in a small intrusion near the Misen pluton.

### Description of the ominelite-bearing rocks

Ominelite is found in porphyritic granite and granodiorite composed mainly of alkali-feldspar, plagioclase, and quartz with lesser amounts of sekaninaite (Fe-dominant analogue of cordierite), biotite and muscovite plus minor andalusite, topaz, garnet, ominelite, dumortierite, schorl, zircon, apatite, monazite, ilmenite, and pyrite. Secondary sericite and chlorite locally replace cordierite, biotite, ominelite, and andalusite, and topaz. A representative bulk chemical composition of ominelite-bearing rock (Sp. 98052906B) is SiO<sub>2</sub> 76.19, TiO<sub>2</sub> 0.08, Al<sub>2</sub>O<sub>3</sub> 2.96, Fe<sub>2</sub>O<sub>3</sub> (total Fe) 1.23, MnO 0.03, MgO 0.10, CaO 0.38, Na<sub>2</sub>O

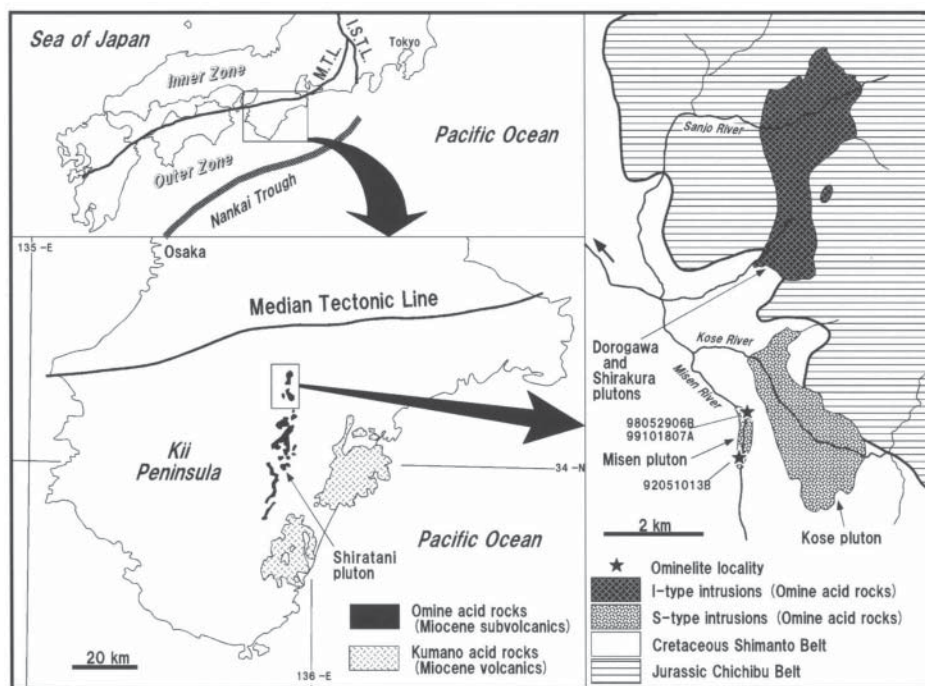


FIGURE 1. Geological sketch maps showing the ominelite locality (modified after Murata 1982; Takahashi 1986; Shiida et al. 1989).

3.06, K<sub>2</sub>O 5.09, P<sub>2</sub>O<sub>5</sub> 0.12, total 99.24 wt%. This composition is close to the minimum melting composition in the H<sub>2</sub>O-saturated system Qz-Ab-Or-H<sub>2</sub>O at 0.5-1 kbar pressures (Tuttle and Bowen 1958).

Ominelite grains range from elongated and euhedral to equant and anhedral and are up to 0.5 mm long. Ominelite is in direct contact with all the other constituent minerals with the exceptions of rare topaz and garnet. Relatively large grains commonly show zoning, in part oscillatory (Figs. 2a and 2b). Ominelite is often partially replaced by tourmaline. Alkali-feldspar, plagioclase, quartz, and sekaninaite occur both as phenocrysts and in the groundmass. Alkali-feldspar commonly shows Carlsbad twin and encloses smaller grains of plagioclase and quartz. It is occasionally intergrown with quartz to make a micrographic texture. Phenocrysts of plagioclase, sekaninaite, and quartz commonly show oscillatory zoning, which is evident in scanning electron microscopy cathodoluminescence images (Fig. 2d). Sector twinning on a sixling pattern is universal in sekaninaite phenocrysts, which are usually free of inclusions. Compositional zoning is observable even under the microscope, and compositional zones within individual sectors usually appear to be straight but a few are curved. Dumortierite occurs as euhedral to subhedral grains up to 1 mm long. Relatively large grains show remarkable zoning, which is displayed as colors ranging from pink through purple to blue. Andalusite occurs as euhedral to anhedral zoned grains. It is occasionally found as euhedral inclusions in sekaninaite phenocrysts. Rare topaz usually occurs as anhedral grains, being closely associated with andalusite. Rare garnet occurs both as anhedral poikilitic microphenocrysts and as euhedral minute grains in the groundmass. Two types of biotite are distinguished. Reddish brown biotite forms microphenocrysts and is present in the groundmass, whereas pale green biotite is associated with muscovite and replaces sekaninaite.

#### Origin of ominelite and conditions estimated for its formation

The origin of Al-rich minerals such as sekaninaite, topaz, andalusite, ominelite, and dumortierite in the Misen pluton raises a question of genesis often encountered in studies of S-type granites. In the case of the Misen pluton, two scenarios are possible for formation of the Al-rich minerals. On one hand, certain petrographic features suggest a magmatic origin, e.g., euhedral outlines of some sekaninaite phenocrysts and ominelite microphenocrysts and oscillatory zoning. Euhedral andalusite sometimes occurs as inclusions in sekaninaite phenocrysts. The enrichment in Al necessary for these minerals to appear on the liquidus can be attributed to an abundance of pelitic sediments in the source rocks for the Omime S-type granites. On the other hand, such petrographic features are also consistent with a restitic origin (e.g., White and Chappell 1977; Chappell et al. 1987). That is, the Al-rich minerals resulted from reaction of minerals such as muscovite and biotite in the source rock with anatectic melt to form sekaninaite, ominelite, and topaz. In most pelitic rocks, Fe/Mg ratios are sufficiently low for the cordierite and grandierite phases to be Mg dominant, and F activities sufficiently low for andalusite or sillimanite to appear instead of topaz. If a restitic origin of the Al-rich minerals is

assumed, the high Fe/Mg ratios in sekaninaite and ominelite and the appearance of topaz could be attributed to the interaction of melt with restitic material. Boron could have originated from the sediments in the source and subsequently been incorporated in the melt and any associated vapor phase; ominelite, dumortierite, and, later, tourmaline resulted from the reaction of boron-enriched melt and/or vapor on restitic material.

Available estimates give rather low *P-T* conditions for crystallization of the plutons. Kawasaki (1981) proposed that granitic rocks in the S-type Shiratani pluton, which is located 23 km south of the Misen pluton (Fig. 1), originated from a magma reservoir at a depth not exceeding 20 km but crystallized at a much shallower depth where water pressures did not exceed 1 kbar at 740 °C. On the basis of the compositions of garnet, biotite and cordierite in quartz-orthoclase aggregates inferred to be refractory residues (restite) and containing also orthopyroxene *or* sillimanite, Murata (1982, 1984) estimated conditions of *T* = 700 °C, *P* = 5 kbar for partial melting that gave rise to the S-type Omime granites south of the Misen pluton. Murata (1982, 1984) also mentioned that some highly differentiated magmas rose to a shallow depth where water pressure was 0.5–1 kbar, resulting in the formation of the Misen and Kose plutons. These estimates are consistent with the presence of andalusite in the Misen pluton, which constrains pressures to not exceed 4 kbar at 500 °C and temperatures to not exceed 750 °C at near-surface conditions (e.g., Holdaway 1971). Another discrepancy is that the H<sub>2</sub>O-saturated granite solidus does not enter the stability field for andalusite determined by Holdaway (1971) and accepted by most investigators. This discrepancy could be resolved by the presence of boron in the melt. For example, the presence of 3% B<sub>2</sub>O<sub>3</sub> in the associated fluid phase and 1% B<sub>2</sub>O<sub>3</sub> in the melt could lower the granite solidus by 45 °C to 675 °C (Pichavant 1981; Dingwell et al. 1996), and andalusite could then coexist with melt. In summary, the presence of andalusite suggests temperatures below 700 °C and pressures below 4 kbars for formation of ominelite and the associated sekaninaite, topaz, andalusite, and dumortierite. If pressures are assumed to have been higher, then even greater amounts of B<sub>2</sub>O<sub>3</sub> in the melt and associated fluid phase must also be assumed for the coexistence of andalusite with a granite melt. In addition, the extreme iron enrichment of ominelite and associated ferromagnesian minerals (see below under mineral compositions) suggests that these minerals formed during the late stage of crystallization of a highly differentiated magma.

#### PHYSICAL AND OPTICAL PROPERTIES

No cleavage is observed in ominelite. Its luster is vitreous and the Mohs hardness is ~7. Its color is blue and the streak is pale blue. The calculated density is 3.169 g/cm<sup>3</sup> for the composition in column 2 of Table 1 and the refined unit-cell parameters reported below.

Ominelite is transparent and blue in thin section; it is biaxial negative. For measurement of optic angles and refractive indices, a single ominelite crystal from sample no. 98052906B approximately 200 μm in diameter was mounted on an X-ray goniometer head and then attached to a Supper spindle stage (Bloss 1981). Measurements at three wavelengths F (486.1 nm),

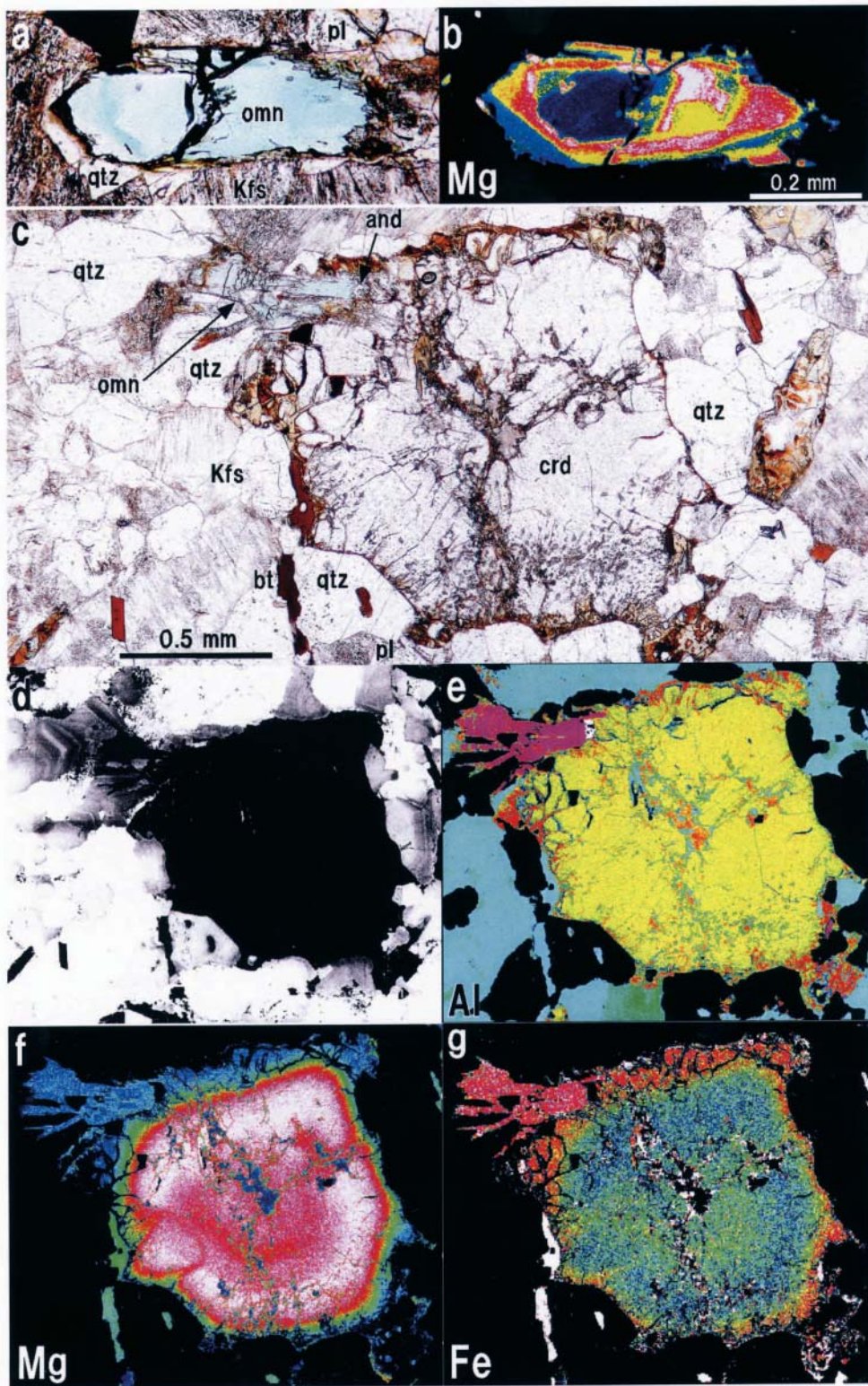


**FIGURE 2.** Images of sample 98052906B. (a) Photomicrograph (plain light) of zoned ominelite (omn) with quartz (qtz) and plagioclase (pl) in alkali feldspar (Kfs). (b) Mg elemental map of (a). (c) Photomicrograph (plain light) of ominelite and andalusite (and) adjacent to sekaninaite-cordierite phenocryst (crd). Bt = biotite. (d) cathodoluminescence image taken with a scanning electron microscope of (c) showing oscillatory zoning in quartz. (e–g) Al, Mg, and Fe elemental maps of (c). In the elemental maps, white indicates the highest concentrations and blue, the lowest.

D (589.3 nm), and C (656.3 nm) were made using the spindle stage method (Bloss 1981; Su et al. 1987) together with dispersion staining techniques (Su 1993, 1998). Optical constants measured at D are  $\alpha = 1.631(1)$ ,  $\beta = 1.654(1)$ ,  $\gamma = 1.656(1)$ ,  $2V_{\text{meas}} = 31.5(6)^\circ$ , and  $2V_{\text{calc}} = 32.5^\circ$ .  $2V_{\text{meas}} = 37.4(9)^\circ$  at F and  $29.9(7)^\circ$  at C, and dispersion is strong,  $v \gg r$ . Pleochroism is  $X = \text{pale blue-green}$ ,  $Y = \text{colorless}$ ,  $Z = \text{pale blue-green}$ .  $Y = c$  (prism elongation direction) so that omnelite, like grandierite, can have either positive or negative sign of elongation and the most intense color perpendicular to the prism length. A calculation using the Gladstone-Dale relationship yields a compatibility index of 0.000 ("superior") for the composition in column 2 of Table 1, the refined unit-cell parameters and the constants tabulated by Mandarino (1981). If the constants for  $^{[4]}\text{Si}$ ,  $^{[5]}\text{Al}$ ,  $^{[6]}\text{Al}$ ,  $^{[4]}\text{Fe}$ ,  $^{[6]}\text{Mg}$ , and  $^{[6]}\text{Mn}$  tabulated by Eggleton (1991) are used instead, the compatibility index worsens somewhat to  $-0.016$  (still "superior").

The average refractive index of grandierite-omnelite increases monotonically with increasing Fe + Mn content and the average index for omnelite lies on the trend set by grandierite (Fig. 3). Our regression of the data gives a somewhat lower slope (0.047) than the 0.053 obtained by Olesch and Seifert (1976), largely because we include three additional samples, all of which are richer in Fe than those plotted by Olesch and Seifert (1976).

### CHEMICAL COMPOSITION

#### Methods

Ominelite was analyzed with a wavelength dispersive JEOL JXA-8800 at the National Science Museum, Japan, by K.

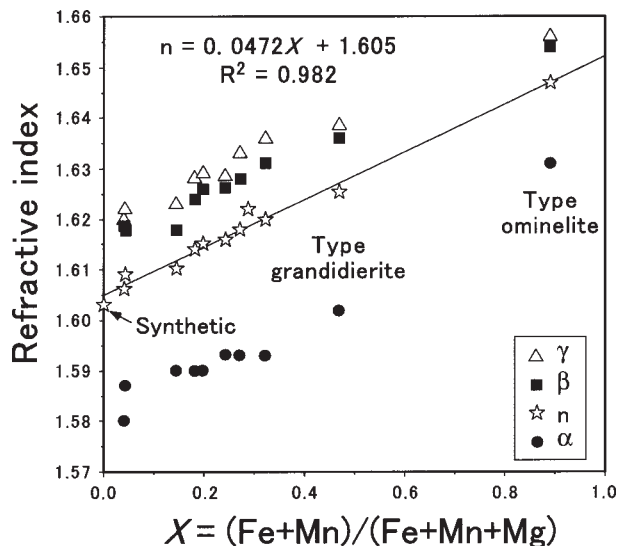


FIGURE 3. Variation of refractive indices and their average [ $n = (\alpha + \beta + \gamma)/3$ ] with total Fe and Mn in grandierite-omnelite, including Fe-free synthetic grandierite. The average has been fitted by linear least squares curve. Data are from McKie (1965), von Knorring et al. (1969), Black (1970), Olesch and Seifert (1976), Anderson (1975), Tan and Lee (1988), Qiu et al. (1990), and this study (sample no. 98052906B). Optical data for type material are from Lacroix (1903), whereas Fe-Mn-Mg data are from Grew et al. (1998); composition of grandierite from type locality is sufficiently uniform to justify combining these data.

TABLE 1. Composition of omnelite

Sample	98052906B		98052906B*		92051013B	
	K. Yokoyama		J.J. McGee		J.J. McGee	
Analyst						
No. of analyses	5		6 except 12 for B		7 except 12 for P, Ti, Ca, F, and 16 for B	
	Average	Range	Average	Range	Average	Range
	Wt%					
SiO <sub>2</sub>	19.22	18.43–19.46	19.34	19.02–19.67	19.18	18.86–19.40
P <sub>2</sub> O <sub>5</sub>	0.21	0.04–0.40	0.13	0.06–0.24	0.13	0.05–0.22
TiO <sub>2</sub>	—	—	0.01	0.00–0.07	0.03	0.00–0.12
Al <sub>2</sub> O <sub>3</sub>	47.98	47.81–48.15	48.85	48.70–48.98	48.35	48.14–48.51
FeO	21.05	20.84–21.48	19.37	19.05–19.89	19.31	18.73–20.05
MnO	0.44	0.41–0.48	0.43	0.30–0.56	0.55	0.29–0.77
MgO	1.20	0.88–1.33	1.33	1.29–1.37	1.37	1.05–1.64
ZnO	0.20	0.13–0.28	—	—	—	—
CaO	—	—	0.01	0.00–0.01	0.01	0.00–0.03
B <sub>2</sub> O <sub>3</sub>	10.69	10.22–11.06	10.91	9.71–11.74	10.23	9.21–10.92
F	—	—	0.01	0.00–0.03	0.01	0.00–0.03
Total	100.99		100.36		99.12	
Formulae per nine O atoms						
Si	1.010		1.011		1.020	
P	0.009		0.006		0.006	
Al	2.971		3.010		3.030	
Fe	0.925		0.847		0.859	
Mn	0.020		0.019		0.025	
Mg	0.094		0.103		0.109	
Zn	0.008		—		—	
B	0.969		0.985		0.939	
Total	6.006		5.982		5.987	
X <sub>Fe</sub>	0.908	0.897–0.910	0.891	0.888–0.896	0.888	0.867–0.915
X <sub>Fe+Mn</sub>	0.910	0.899–0.911	0.893	0.890–0.899	0.891	0.871–0.917

Note: All Fe as FeO. Totals do not include TiO<sub>2</sub>, CaO, and F. X<sub>Fe</sub> = Fe/(Fe + Mg); X<sub>Fe+Mn</sub> = (Fe + Mn)/(Fe + Mn + Mg).

\* Indicates Grain 1. Grain 2 of this sample was used for structure refinement.

Yokoyama. Standards were synthetic  $Mg_2SiO_4$  (Mg), synthetic  $Fe_2SiO_4$  (Fe), sillimanite (Al), danburite (Si and B), synthetic GaP (P), Mn metal (Mn), and Zn metal (Zn). All the analyses were done at an accelerating voltage of 15 kV, a beam current of 20 nA, and at a spot size of 5  $\mu m$ . Peaks and backgrounds were measured for 30 and 15 seconds, respectively, for Mg, Fe, Al, and Si, and 50 and 30 seconds, respectively, for B. The  $\phi\rho(Z)$  method was used for the corrections. The analyses have been averaged over single grains and presented in column 1 of Table 1. The minerals associated with ominelite were analyzed with a JEOL JXA-8800 using similar standards, analytical conditions, and corrections at the National Institute of Polar Research (NIPR), Japan, by Y. Motoyoshi, T. Hokada, and Y. Hiroi. These analyses are presented in Table 2.

Measurements by J.J. McGee at the University of South Carolina (USC) were made with a wavelength-dispersive Cameca SX50 electron microprobe at 10 kV, 50 to 100 nA probe (cup) current, and a 1–2  $\mu m$  spot size. Boron was measured concurrently with the other constituents using an ODPb (lead

stearate) crystal and measurement was made “on peak” (as opposed to peak area integration). Counting times were 90 seconds for boron and 30 seconds for the other elements. Danburite was chosen as the best B standard available for mineralogical analysis. The higher B content in danburite was especially useful for calibration of the ODPb crystal, which has a significantly lower count yield than synthetic multilayer crystals. For the other constituents, the following standards were used: F = F-phlogopite (synthetic), Na = plagioclase (Lake Co., USNM 115900), P = Durango apatite (USNM 104021), Mn = Ilmen ilmenite (USNM 96189), K = microcline (USNM 143966), and Mg, Al, Si, Ca, Ti, Fe = Kakanui hornblende (USNM 143965). Two sections of ominelite-bearing rock were analyzed, nos. 98052906B and 92051013B. These had been mounted in a medium that permitted ready extraction of crystals for crystallographic study. Unfortunately, this created difficulties for the analyses. Analytical totals were low in several runs, but a few analyses gave reasonable totals and stoichiometries. These analyses were averaged over single grains and presented in Table 1.

**TABLE 2.** Representative analyses of minerals associated with ominelite

Mineral sample	And 9910180 7A	Topz 9910180 7A	Dmt 9805290 6B	Pl 9805290 6B	Kfs 9805290 6B	Crd 9805290 6B	Gar 9205101 3A	Bt-1 9805290 6B	Bt-2 9805290 6B	Mus 9805290 6B	Tur 9805290 6B	Ilm 9805290 6B	Ap 9805290 6B
SiO <sub>2</sub>	36.46	32.17	30.31	66.33	65.37	45.98	36.20	33.42	35.60	47.76	35.12	0.02	0.00
TiO <sub>2</sub>	0.06	0.06	2.27	0.03	0.00	0.00	0.16	2.13	0.65	0.15	0.00	53.01	0.00
Al <sub>2</sub> O <sub>3</sub>	62.24	54.72	59.06	21.35	18.77	31.71	20.25	21.17	21.93	35.34	33.63	0.01	0.02
Cr <sub>2</sub> O <sub>3</sub>	0.00	0.07	0.05	0.00	0.00	0.00	0.00	0.02	0.04	0.01	0.02	0.00	0.06
FeO*	0.36	0.00	0.49	0.00	0.00	17.33	36.12	26.25	24.81	2.92	14.16	43.95	1.58
MnO	0.03	0.01	0.00	0.01	0.00	0.85	5.64	0.25	0.29	0.00	0.31	2.05	1.52
MgO	0.00	0.00	0.15	0.01	0.00	1.14	0.40	1.74	1.93	0.10	0.93	0.00	0.04
CaO	0.01	0.00	0.01	1.51	0.05	0.01	0.50	0.00	0.03	0.00	0.00	0.00	51.76
Na <sub>2</sub> O	0.01	0.02	0.00	10.73	2.39	0.42	0.03	0.19	0.19	0.54	1.97	0.00	0.17
K <sub>2</sub> O	0.00	0.02	0.01	0.46	13.57	0.00	0.02	9.24	9.50	8.89	0.00	0.00	0.00
P <sub>2</sub> O <sub>5</sub>	0.05	0.13	0.06	0.33	0.22	0.01	0.11	0.03	0.05	0.05	0.30	0.00	41.86
F		20.03	0.03					1.23	1.52	1.26	0.18	0.00	3.42
Cl		0.02	0.00					1.08	0.91	0.13	0.03	0.00	0.47
B <sub>2</sub> O <sub>3</sub> *			6.09								10.34		
H <sub>2</sub> O*			1.17					2.92	2.90	3.93	3.48		0.02
O=F,Cl		-8.44	-0.01					-0.76	-0.85	-0.56	-0.08	0.00	-1.55
Total	99.22	98.81	99.68	100.75	100.37	97.45	42.82	98.90	99.50	100.52	100.38	99.04	99.38
O	5	5	18	8	8	18	24	22	22	22	31	3	13
Si	0.994	0.996	2.887	2.892	2.981	5.005	5.998	5.313	5.545	6.287	5.903	0.000	0.000
B			1.000								3.000		
Ti	0.001	0.001	0.163	0.001	0.000	0.000	0.020	0.255	0.076	0.015	0.000	1.011	0.000
Al	1.999	1.996	6.630	1.097	1.009	4.068	3.955	3.967	4.026	5.483	6.662	0.000	0.002
Cr	0.000	0.002	0.004	0.000	0.000	0.000	0.000	0.003	0.005	0.001	0.003	0.000	0.004
Fe	0.008	0.000	0.039	0.000	0.000	1.577	5.005	3.490	3.232	0.321	1.991	0.932	0.112
Mn	0.001	0.000	0.000	0.000	0.000	0.078	0.792	0.034	0.038	0.000	0.044	0.044	0.109
Mg	0.000	0.000	0.021	0.000	0.000	0.185	0.099	0.412	0.448	0.020	0.233	0.000	0.005
Ca	0.000	0.000	0.001	0.071	0.002	0.001	0.089	0.000	0.005	0.000	0.000	0.000	4.716
Na	0.001	0.001	0.000	0.907	0.211	0.089	0.010	0.059	0.057	0.138	0.642	0.000	0.028
K	0.000	0.001	0.001	0.026	0.789	0.000	0.004	1.874	1.888	1.493	0.000	0.000	0.000
P	0.001	0.003	0.005	0.012	0.008	0.001	0.015	0.003	0.007	0.006	0.043	0.000	3.014
F	0.000	1.960	0.009	0.000	0.000	0.000	0.000	0.618	0.749	0.525	0.096	0.000	0.920
Cl	0.000	0.001	0.000	0.000	0.000	0.000	0.000	0.291	0.240	0.029	0.009	0.000	0.068
H			0.741					3.091	3.011	3.446	3.896		0.012
Total cations	3.004	3.000	10.751	5.006	5.002	11.004	15.987	15.409	15.326	13.763	18.521	1.987	7.991
X <sub>Fe</sub>	—	—	0.647	—	—	0.895	0.981	0.894	0.878	0.942	0.895	1.000	0.957
X <sub>Fe+Mn</sub>			0.647			0.899	0.983	0.895	0.879	0.942	0.897	1.000	0.978
an				0.070	0.002								
ab				0.904	0.211								
or				0.026	0.787								

Note: All Fe as FeO.  $X_{Fe} = Fe/(Fe + Mg)$ ;  $X_{Fe+Mn} = (Fe + Mn)/(Fe + Mn + Mg)$ .

\*B<sub>2</sub>O<sub>3</sub> and H<sub>2</sub>O were calculated assuming ideal stoichiometry: 1.0B and 0.75(OH,F) for dumortierite, 3.0B and 4(OH,F) for tourmaline, 4(OH,F,Cl) for biotite and muscovite, and 1(F,Cl,OH) for apatite.

### Ominelite

The only constituents detected in measurable amounts with the electron microprobe are Si, Al, B, Zn, P, Fe, Mn, and Mg (Table 1). The probe analyses give a stoichiometry approaching the ideal  $(\text{Fe,Mg,Mn})\text{Al}_3\text{BSiO}_9$ , which is consistent with the refined site occupancies from the single crystal X-ray study (see below). Deficiency in B in the electron microprobe analyses could result from any of the many analytical problems discussed by McGee and Anovitz (1996). An example is the use of an analyzing crystal of very low count rate yield at USC. The significance of ZnO and  $\text{P}_2\text{O}_5$  is not clear. ZnO was only found in analyses done at the National Science Museum; qualitative line scans at USC failed to detect it. The phosphorus content ranges from 0 to 0.55 wt%  $\text{P}_2\text{O}_5$  in individual analyses on all three probes, and elemental images of P show a distinct zoning, implying that the presence of P must be real, not an artifact of the electron microprobe analytical method. Presumably, P would substitute for Si, but no correlation between P and Si was found in 54 analyses done at NIPR, in which average Si =  $0.996 \pm 0.016$  and average P =  $0.008 \pm 0.007$  per 7.5 O, assuming ideal B. Ominelite is heterogeneous in terms of the major compositional variables Mg, Mn, and Fe, both from sample to sample and within a sample; grains are markedly zoned (Figs. 2a and 2b). In individual analyses  $X_{\text{Fe}}$  ranges from 0.542 to 0.945 overall, and in the Misen pluton,  $X_{\text{Fe}}$  is near 0.90. Overall, the Mn/(Fe + Mn + Mg) ratio ranges from 0.012 to 0.033. The latter corresponds to 0.73 wt% MnO; the highest amount previously reported for grandidierite was 0.37 wt% (Grew 1996). In general, the Mn content varies independently of the Fe content.

### Cordierite-sekaninaite

Cordierite-sekaninaite  $X_{\text{Fe}}$  overall ranges in individual analyses from 0.463 to 0.982 and the Mn/(Fe + Mn + Mg) ratio from 0.013 to 0.065; the Mn and Fe contents are positively correlated. In the Misen pluton, cordierite phenocrysts larger than 1 mm in diameter and free of inclusions, with the exception of the outermost part, show a distinctive zoning;  $X_{\text{Fe}}$  reaches 0.62 at the core, decreases to a minimum near 0.52 toward the rim, and then increases to 0.90 in the outermost rim (Fig. 2g). The rim composition varies from spot to spot in a single phenocryst and also differs from one phenocryst to another. The maximum  $X_{\text{Fe}}$  found was 0.92.

### Other minerals

Ferromagnesian silicates approach their respective Fe end-members with considerable Mn enrichment (e.g., Table 2). Biotites are titanian siderophyllite, with  $X_{\text{Fe}}$  ranging from 0.592 to 0.905 and with significant F and Cl. Topaz approaches the F end-member. Phosphorus was found in dumortierite and feldspar, with a small preference for plagioclase over K-feldspar. Although in general K-feldspar contains more P than plagioclase (Cerný 1994), London (1992) found that fractionation of P is small between co-precipitating feldspars.

### CRYSTAL STRUCTURE

Powder X-ray data were obtained from sample 98052906B with a Gandolfi camera (114.6 mm) using  $\text{CuK}\alpha$  radiation at

the National Science Museum, Japan (Table 3).

A crystal fragment was removed from a thin section of sample 98052906B and used for single-crystal X-ray diffraction studies at the University of Michigan. Although it had not been analyzed by the electron microprobe, another crystal from that same thin section had been analyzed (Table 1). Precession and Weissenberg photographs verified that the space group is *Pbnm* (a non-standard setting of *Pnma*) identical to that found by Stephenson and Moore (1968) for grandidierite, and later verified by the presence or absence of reflections in the full set of intensities. Lattice parameters, determined using measurements from photographs and refined using the setting angles of 25 reflections measured with an Enraf-Nonius CAD4 four-circle diffractometer, are  $a = 10.343(2)$ ,  $b = 11.095(1)$ ,  $c = 5.7601(8)$  Å,  $V = 661.0(2)$  Å<sup>3</sup>. The intensities of 1415 reflections in one octant of reciprocal space to a maximum  $2\theta$  of 65° were then measured. Of these, 1122 having  $I > 2\sigma(I)$  were considered observed. Starting with the atomic parameters of grandidierite reported by Stephenson and Moore (1968), the structure model refined smoothly to unweighted residuals of 0.032 and 0.023 with isotropic and anisotropic atomic displacement factors, respectively. No evidence of extinction error was observed among the intense low-theta reflections. A final difference electron-density synthesis showed no maxima greater than 0.71 e/Å<sup>3</sup>. Additional details of the intensity data collection and structure refinement are given in Table 4, structure factors in Table 5<sup>1</sup>, refined atomic coordinates and equivalent isotropic displacement factors in Table 6, anisotropic displacement factors in Table 7, selected interatomic distances and angles in Table 8, and calculated empirical bond valences in Table 9. These data are confirmed by crystal structure analysis of the type material at the National Science Museum, Japan.

Refinement of the site occupancy factor of Fe in the  $(\text{Fe}^{2+}, \text{Mg})$  site yielded 3.707(7) Fe + 0.293 Mg atoms, or 92.68% Fe and 7.32% Mg, which corresponds closely to the value of 89.3% (including Mn with Fe) obtained by electron microprobe analysis. The total occupancy factors of the three Al sites were also refined to test the possibility of (Al, Fe<sup>3+</sup>) solid solution. The results are 3.938(8) Al at Al1, 3.999(8) Al at Al2, and 4.008(8) Al at Al3. The value for Al1 is consistent with only slightly less electron density than can be accommodated by Al, and is therefore incompatible with solid solution of Fe on that site. The values for Al2 and Al3 are equal to that required for full occupancy by Al, within error. Additionally, Al1-O, Al2-O, and Al3-O are consistent with full occupancy by aluminium. The occupancies of all three Al sites were therefore fixed at 4 Al atoms in the final cycles of refinement.

Ominelite (Fig. 4) is isostructural with grandidierite (Stephenson and Moore 1968), and thus belongs to the family of B-Al-Si phases that includes boralsilite, andalusite, sillimanite, werdingite, synthetic  $\text{Al}_8[(\text{Al},\text{B})_{12}\text{B}_4]\text{O}_{33}$ , and mullite. All

<sup>1</sup>For a copy of Table 5, Document AM-01-001, contact the Business Office of the Mineralogical Society of America (see inside front cover of recent issue) for price information. Deposit items may also be available on the American Mineralogist web site at <http://www.minsocam.org> or current web address.

**TABLE 3.** Powder X-ray diffraction data and lattice parameters of ominelite and grandierite

h	k	l	Ominelite Omine, Japan (Present study)			Grandierite Sakatelo, Madagascar (McKie 1965)	
			l	d(obs)	d(calc)	l	d(obs)
			w	9.94	*		
			vvw	7.56	*		
			vw	7.05	†		
0	2	0	m	5.57	5.56	vs	5.482
2	0	0	vs	5.21	5.18	vvs	5.17
1	0	1	vvs	5.05	5.04	vvs	5.04
1	2	0	vvw	4.89	4.90	w	4.84
2	1	0	vw	4.69	4.70		
1	1	1	vwb	4.50	4.59	vw	4.59
0	2	1			4.01	vw	3.97
2	2	0	w	3.79	3.79	vw	3.75
1	2	1	m	3.73	3.74	ms	3.708
1	3	0	m	3.51	3.49	w	3.449
			vw	3.34‡			
3	1	0			3.30	vw	3.29
2	2	1	vw	3.18	3.17	w	3.150
2	3	0			3.02	vw	2.99
3	0	1	s	2.97	2.96	m	2.956
3	2	0	vvw	2.93	2.93	vw	2.92
0	0	2	m	2.90	2.88	w	2.878
3	1	1			2.86	vw	2.855
0	4	0	s	2.79	2.78	vs	2.744
1	4	0	vw	2.69	2.69	vwb	2.66
2	3	1			2.67		
3	2	1	m	2.62	2.62	m	2.602
4	0	0			2.59	ms	2.584
0	2	2	m	2.56	2.56	mw	2.551
4	1	0			2.52	w	2.515
2	0	2	w	2.53	2.52		
0	4	1			2.51	vwb	2.48
2	1	2	vw	2.46	2.46		
1	4	1			2.44	vwb	2.41
4	2	0	vvw	2.35	2.35	vw	2.337
2	2	2	w	2.30	2.30	mw	2.287
1	3	2	vvw	2.22	2.22	mw	2.210
1	5	0			2.18	m	2.149
4	2	1	s	2.18	2.18	s	2.166
3	1	2			2.17		
2	3	2			2.09	vw	2.072
3	2	2	vvw	2.06	2.06	vw	2.050
2	5	0			2.05		
5	1	0			2.04	mw	2.031
1	5	1	w	2.03	2.04	vwb	2.012
3	4	1			2.03		
5	0	1	w	1.952	1.951	mw	1.946
5	1	1	m	1.924	1.921		
1	0	3	m	1.890	1.891		
2	4	2	vvw	1.865	1.868		
1	1	3			1.864		
0	6	0	vvw	1.855	1.855		
5	3	0	vvw	1.811	1.809		
2	6	0			1.746		
1	6	1	vwb	1.740	1.741		
1	5	2			1.737		
3	0	3	vvw	1.674	1.680		
2	6	1			1.671		
5	1	2	vvw	1.666	1.664		

these phases have structures based on chains of edge-sharing Al octahedra parallel to a lattice translation of ca. 5.6 Å, which is the *c*-axis in the case of ominelite and grandierite. According to Peacor et al. (1999) the phases in this family differ from one another in the nature of the polyhedral units cross-linking the octahedral Al chains. In ominelite, shared edges in the Al1 and Al2 octahedral chains are defined by O2-O3 and O4-O5, respectively. The interchain spaces are occupied by B with planar-trigonal coordination, tetrahedrally coordinated Si, and a

**TABLE 3—continued**

h	k	l	Ominelite Omine, Japan (Present study)			Grandierite Sakatelo, Madagascar (McKie 1965)	
			l	d(obs)	d(calc)	l	d(obs)
6	2	0	vvw	1.651	1.650		
3	6	0	vvw	1.632	1.634		
3	2	3	vwb	1.609	1.609		
4	4	2	vwb	1.584	1.584		
0	4	3					1.582
6	3	0	vwb	1.563			1.566
0	6	2					1.560
5	3	2	vvw	1.531	1.533		
6	0	2	m	1.483	1.482		
2	7	1					1.47
6	1	2	vvw	1.471	1.469		
7	1	0					1.468
4	6	1	vvw	1.457	1.459		
0	0	4	m	1.443	1.442		
0	8	0	vw	1.389	1.391		
2	0	4					1.389
6	3	2	vvw	1.378	1.376		
3	5	3					1.341
7	3	1	vwb	1.341	1.338		
4	6	2					1.337
6	4	2	w	1.306	1.308		
6	6	0					1.264
8	2	0	vw	1.261	1.262		
3	8	1					1.259
			a	= 10.363(5) Å		a	= 10.335 Å
			b	= 11.129(5) Å		b	= 10.978 Å
			c	= 5.769(3) Å		c	= 5.760 Å

\* Diffraction from biotite.

† Diffraction from chlorite.

‡ Diffraction from quartz.

**TABLE 4.** Experimental details

Crystal size	0.07 × 0.22 × 0.17 mm
Data measurement	
Radiation	Monochromatized MoK $\alpha$
Index limits	0 ≤ h ≤ 15, 0 ≤ k ≤ 16, 0 ≤ l ≤ 8
Maximum 2 $\theta$	65°
Scan type	$\omega/2\theta$
Scan rates	0.4° to 5.5°/min in $\omega$
Scan widths	0.78 + 0.35 tan $\theta$
Intensity monitoring	3 reflections every 3 hrs
Orientation monitoring	3 reflections every 400 reflections
Data corrections	Lorentz, polarization, and absorption ( $\mu = 27.3 \text{ cm}^{-1}$ ) effects
Structure refinement	
Type	Full-matrix least-squares
Function minimized	$\sum w ( F _{\text{obs}} -  F _{\text{cal}})^2$
Reflection weights	$4 F^2_{\text{obs}} / \sigma^2 (F^2_{\text{obs}})$
Anomalous dispersion	For all atoms
Observations	1133 reflections with $I > 2 \sigma(I)$
Variables	86
R (observed data)	0.023
w R (observed data)	0.031
R (all data)	0.033
Esd obs. of unit wt.	1.360
Largest shift/error	0.00
Largest $\Delta\rho$ (x, y, z)	+0.71 and -0.18 e/Å <sup>3</sup>
Diffraction	Enraf-Nonius CAD4
Crystallographic software	MolEN System

dimer of edge-sharing five-coordinated Fe and Al3 polyhedra. The triangular plane of oxygen atoms coordinating B is shown only as a line in Figure 4, as it is oriented perpendicular to the plane of the diagram, with two superimposed B-O7 bonds (represented as a bold line) to adjacent, edge-sharing Al2 octahedra and one (B-O6) bond to an Al1 octahedron. Although fivefold coordination polyhedra are relatively unusual in mineral structures, they are a common building block of this family of structures. A similar unit consisting of the dimer plus SiO<sub>4</sub> and BO<sub>3</sub> polyhedra occurs in the boralsilite structure, although in the latter case a dimer of trigonal bipyramids becomes a trimer with the addition of a third AlO<sub>5</sub> group.

The dimer in ominelite includes the fivefold-coordinated polyhedron about Al3, which approximates a trigonal bipyramid (Fig. 5a). A potential bond to a sixth ligand, O4, is very long, 2.831 Å, and beyond the limits of normal inclusion in the coordination polyhedron; thus Al3 is not considered to be six-coordinated. The long axis of the other polyhedron of the dimer, the distorted trigonal bipyramid about the (Fe,Mg) site, is defined by the nearly parallel (Fe,Mg)-O2 and (Fe,Mg)-O5 bonds, both of which are nearly parallel to the **b** axis (Fig. 5b). These two bonds are much longer in ominelite, 2.228 and 2.111 Å, respectively, than in Mg-dominant grandidierite, 2.176 and 2.054 Å. The three other (Fe,Mg)-O bonds of the trigonal

**TABLE 8.** Selected interatomic distances (Å) and angles (°) in ominelite

Al1-O6	1.889 (1) ×2	Al2-O5	1.857 (1) ×2
O2	1.896 (1) ×2	O7	1.888 (1) ×2
O3	1.908 (1) ×2	O4	1.993 (1) ×2
Mean	1.898	Mean	1.913
Al3-O2	1.794 (2)	O5-Al3-O7	80.45 (4) ×2
O1	1.824 (2)	O1-Al3-O5	91.86 (7)
O7	1.861 (1) ×2	O2-Al3-O7	95.25 (4) ×2
O5	1.931 (1)	O1-Al3-O2	99.27 (7)
Mean	1.854	O1-Al3-O7	112.02 (3) ×2
O4	2.831 (2)	O7-Al3-O7	132.18 (7)
		O2-Al3-O5	168.87 (7)
Fe-O6	1.978 (1) ×2	O2-Fe-O6	77.19 (4) ×2
O1	2.042 (1)	O1-Fe-O5	81.04 (5)
O5	2.111 (1)	O5-Fe-O6	97.98 (4) ×2
O2	2.228 (1)	O6-Fe-O6	105.86 (6)
Mean	2.067	O1-Fe-O2	107.24 (5)
		O1-Fe-O6	126.95 (3) ×2
		O2-Fe-O5	171.73 (5)
Si-O6	1.615 (1) ×2	O1-Si-O6	106.45 (5) ×2
O4	1.625 (2)	O6-Si-O6	107.52 (8)
O1	1.657 (2)	O4-Si-O6	110.53 (5) ×2
Mean	1.628	O1-Si-O4	114.99 (8)
		Mean	109.41
B-O3	1.346 (2)	O7-B-O7	118.26 (17)
O7	1.375 (1) ×2	O3-B-O7	120.86 (9) ×2
Mean	1.365	Mean	119.99

**TABLE 6.** Positional and equivalent isotropic displacement (Å<sup>2</sup>) parameters in ominelite

	x	y	z	B (Å <sup>2</sup> )
Al1	0	0	0	0.374 (9)
Al2	1/2	0	0	0.409 (9)
Al3	0.22671 (5)	0.44837 (5)	1/4	0.362 (8)
Fe	0.09578 (3)	0.21909 (3)	1/4	0.554 (4)
Si	0.43503 (5)	0.26359 (5)	1/4	0.397 (7)
B	0.2510 (2)	0.0003 (2)	3/4	0.44 (3)
O1	0.2775 (1)	0.2910 (1)	1/4	0.65 (2)
O2	0.1174 (1)	0.0193 (1)	1/4	0.45 (2)
O3	0.1210 (1)	0.9957 (1)	3/4	0.55 (2)
O4	0.4742 (1)	0.1217 (1)	1/4	0.55 (2)
O5	0.5463 (1)	0.0963 (1)	3/4	0.44 (2)
O6	0.99337 (9)	0.16972 (9)	0.9761 (2)	0.62 (2)
O7	0.18077 (9)	0.50115 (8)	0.9548 (2)	0.59 (1)

**TABLE 9.** Empirical bond valences (v. u.) in ominelite\*

	Al1	Al2	Al3	Fe	Si	B	Σv <sub>a</sub>
O1			0.627	0.431	0.915		1.973
O2	0.516 (×2)		0.679	0.261			1.972
O3	0.499 (×2)					1.070	2.068
						1.070↓	
O4		0.397 (×2)	0.041		0.997		1.832
O5		0.573 (×2)	0.469	0.358			1.973
O6	0.526			0.513	1.025		2.064
	0.526↓			0.513↓	1.025↓		
O7		0.527	0.567			0.989	2.083
		0.527↓	0.567↓				
?v <sub>c</sub>	3.082	2.994	2.950	2.076	3.962	3.129	

\*Calculated using the bond-valence constants of Brese and O'Keeffe (1991). The sums include the small contribution from the potential bond between Al3 and O4.

**TABLE 7.** Anisotropic displacement parameters (Å<sup>2</sup>) in ominelite

	U <sub>11</sub>	U <sub>22</sub>	U <sub>33</sub>	U <sub>12</sub>	U <sub>13</sub>	U <sub>23</sub>
Al1	0.0048 (2)	0.0056 (2)	0.0038 (2)	0.0003 (2)	-0.0001 (2)	0.0000 (2)
Al2	0.0041 (2)	0.0074 (2)	0.0041 (2)	-0.0003 (2)	0.0000 (2)	0.0009 (2)
Al3	0.0039 (2)	0.0061 (2)	0.0038 (2)	-0.0003 (2)	0	0
Fe	0.0084 (1)	0.0062 (1)	0.0065 (1)	-0.00174 (9)	0	0
Si	0.0056 (2)	0.0045 (2)	0.0050 (2)	-0.0001 (2)	0	0
B	0.0052 (7)	0.0072 (8)	0.0041 (8)	0.0003 (6)	0	0
O1	0.0052 (5)	0.0070 (5)	0.0123 (6)	0.0011 (5)	0	0
O2	0.0054 (5)	0.0069 (5)	0.0047 (5)	0.0004 (4)	0	0
O3	0.0044 (5)	0.0106 (6)	0.0057 (6)	-0.0002 (4)	0	0
O4	0.0091 (5)	0.0054 (5)	0.0062 (5)	0.0011 (5)	0	0
O5	0.0061 (5)	0.0052 (5)	0.0053 (5)	0.0000 (4)	0	0
O6	0.0109 (4)	0.0062 (4)	0.0063 (4)	-0.0003 (3)	-0.0022 (3)	0.0002 (3)
O7	0.0048 (3)	0.0129 (4)	0.0047 (4)	0.0002 (3)	0.0000 (3)	0.0007 (3)

Note: The form of the anisotropic displacement parameter is  $\exp[-2\pi^2\{h^2a^2U_{11} + k^2b^2U_{22} + l^2c^2U_{33} + 2hkabU_{12} + 2hlacU_{13} + 2klbcU_{23}\}]$ , where *a*, *b*, and *c* are reciprocal lattice constants.

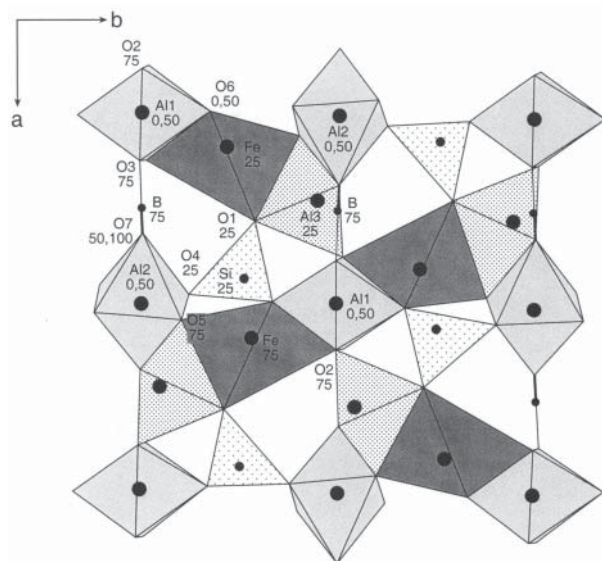


FIGURE 4. Diagram of the crystal structure of ominelite projected parallel to the *c* axis. The *z* coordinate(s)  $\times 100$  are given for each cation. Light gray = Al octahedra; dark gray = Fe trigonal bipyramid; coarse stippling = Si tetrahedron; fine stippling = Al3 trigonal bipyramid. The plane of the trigonal planar polyhedron about B is normal to the diagram, and therefore shown as a line, the bold line corresponding to two superimposed B-O bonds. The Al1 and Al2 atoms occupy inversion centers.

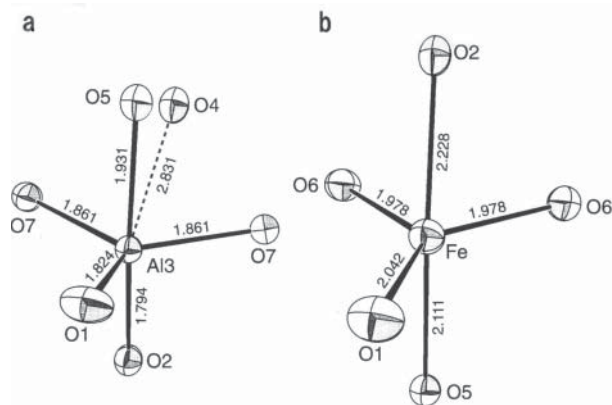


FIGURE 5. Coordination polyhedra. (a) Fivefold-coordinated polyhedron about Al3; (b) nearly parallel (Fe,Mg)-O2 and (Fe,Mg)-O5 bonds, which are nearly parallel to the *b* axis.

bipyramid are nearly of identical length in both structures, as are other polyhedral bond lengths. Lengthening of the (Fe,Mg)-O2 and (Fe,Mg)-O5 bonds with increasing Fe content explains the monotonic increase of *b* with the (Fe + Mn)/(Fe + Mn + Mg) ratio in natural granddierite-ominelite solid solutions, whereas *a* increases much less and *c* almost not at all (Fig. 6). These variations were also noted by Olesch and Seifert (1976). However, cell parameters for the end-member granddierite synthesized by Olesch and Seifert (1976) and by Heide (1992) lie below the trends for the natural materials.

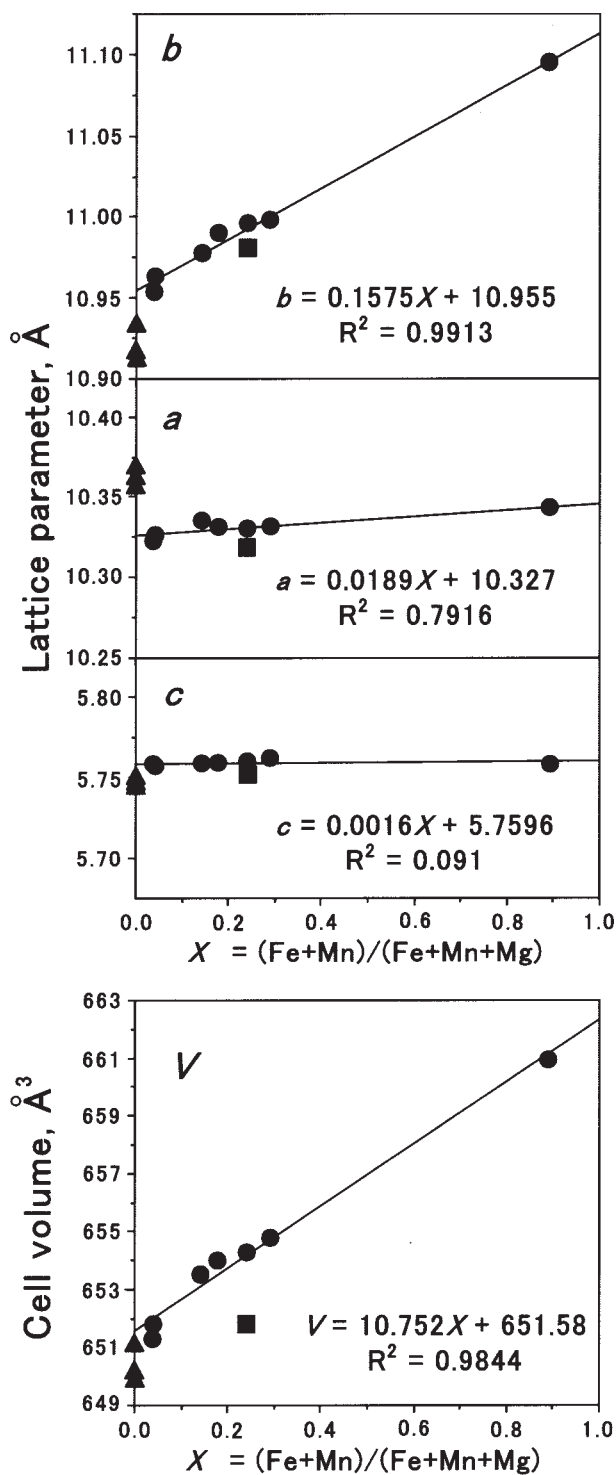


FIGURE 6. Variation of cell parameters and volume with total Fe and Mn in granddierite-ominelite, including Fe-free synthetic granddierite (triangles). Data are from McKie (1965), von Knorring et al. (1969), Olesch and Seifert (1976), Seifert and Olesch (1977), Tan and Lee (1988), Qiu et al. (1990), Heide (1992), and this study (sample no. 98052906B). Two sets of data from Tan and Lee (1988) at (Fe + Mn)/(Fe + Mn + Mg) = 0.25: single-crystal (square) and powder (filled circle). Least squares fit was calculated only for the filled circles.

## ACKNOWLEDGMENTS

Y.H.'s research was supported by the Grant-in-Aid for Scientific Research by the Japanese Ministry of Education, Culture and Science (10304042). E.S.G.'s research was supported by U.S. National Science Foundation grants EAR-9526403 and OPP-9813569 to the University of Maine, and the crystallographic work has been supported by National Science Foundation grants EAR 9418108 and 9814391 to D.R. Peacor. We thank D.M. Carmichael for the first introduction of grandidierite mineral to Y.H., J.G. Liou for the translation of Tan and Lee (1988), and W. Schreyer for a copy of those pages from Heide (1992) relevant to grandidierite cell parameters. We thank C.L. Cahill and R.J. Swope for their constructive reviews.

## REFERENCES CITED

- Anderson, S.M. (1975) Grandidierite and kornepurine: two boron-bearing minerals new to Rhodesia. *Annals of the Rhodesian Geological Survey*, 1, 49–59.
- Black, P.M. (1970) Grandidierite from Cuvier Island, New Zealand. *Mineralogical Magazine*, 37, 615–617.
- Blass, G. and Graf, H.-W. (1994) Über neue Mineralien vom Bellerberg, Eifel. *Mineralien Welt*, 5(6), 53–55.
- Bloss, F.D. (1981) *The Spindle Stage: Principles and Practice*, 340 p. Cambridge University Press, Cambridge.
- Breese, N.E. and O'Keefe, M. (1991) Bond-valence parameters for solids. *Acta Crystallographica*, B47, 192–197.
- Cerny, P. (1994) Evolution of feldspars in granitic pegmatites. In I. Parsons, Ed., *Feldspars and Their Reactions*, p. 501–540. Kluwer, Dordrecht.
- Chappell, B.W. and White, A.R.J. (1974) Two contrasting granite types. *Pacific Geology*, 8, 173–174.
- Chappell, B.W., White, A.R.J., and Wyborn, D. (1987) The importance of residual source material (restite) in granite petrogenesis. *Journal of Petrology*, 28, 1111–1138.
- Dingwell, D.B., Pichavant, M., and Holtz, F. (1996) Experimental studies of boron in granitic melts. In *Mineralogical Society of America Reviews in Mineralogy*, 33, 331–385.
- Eggleton, R.A. (1991) Gladstone-Dale constants for the major elements in silicates: Coordination number, polarizability, and the Lorentz-Lorentz relation. *Canadian Mineralogist*, 29, 525–532.
- Grant, J.A. and Frost, B.R. (1990) Contact metamorphism and partial melting of pelitic rocks in the aureole of the Laramie Anorthosite Complex, Morton Pass, Wyoming. *American Journal of Science*, 290, 425–472.
- Greenfield, J.E., Clarke, G.L., and White, R.W. (1998) A sequence of partial melting reactions at Mt Stafford, central Australia. *Journal of Metamorphic Geology*, 16, 363–378.
- Grew, E.S. (1996) Borosilicates (exclusive of tourmaline) and boron in rock-forming minerals in metamorphic environments. In L.M. Anovitz and E.S. Grew, Eds., *Boron: Mineralogy, Petrology and Geochemistry*, 33, 387–502. *Reviews in Mineralogy, Mineralogical Society of America*, Washington, D.C.
- Grew, E.S., Yates, M.G., Huijsmans, J.P.P., McGee, J.J., Shearer, C.K., Wiedenbeck, M., and Rouse, R.C. (1998) Werdingite, a borosilicate new to granitic pegmatites. *Canadian Mineralogist*, 36, 399–414.
- Hasebe, N., Suwagardi, B.W., and Nishimura, S. (2000) Fission track ages of the Omime acid rocks, Kii Peninsula, Southwest Japan. *Geochemical Journal*, 34, 229–235.
- Heide, M. (1992) *Synthese und Stabilität von Grandidierit, MgAl<sub>3</sub>BSiO<sub>9</sub>*. Diplomarbeit, Ruhr-Universität Bochum, 90 p.
- Herd, R.K., Windley, B.F., and Ackermann, D. (1984) Grandidierite from a pelitic xenolith in the Haddo House complex, NE Scotland. *Mineralogical Magazine*, 48, 401–406.
- Holdaway, M.J. (1971) Stability of andalusite and the aluminum silicate phase diagram. *American Journal of Science*, 271, 97–131.
- Huijsmans, J.P.P., Barton, M., and van Bergen, M.J. (1982) A pegmatite containing Fe-rich grandidierite, Ti-rich dumortierite and tourmaline from the Precambrian, high-grade metamorphic complex of Rogaland, S.W. Norway. *Neues Jahrbuch für Mineralogie Abhandlungen*, 143, 249–261.
- Kawasaki, M. (1980a) Omime acid rocks, Kii Peninsula – Geology and major element chemistry. *Journal of the Japanese Association of Mineralogists, Petrologists, and Economic Geologists*, 75, 86–102.
- (1980b) Omime acid rocks, Kii Peninsula—Mineralogy. *Journal of the Japanese Association of Mineralogists, Petrologists, and Economic Geologists*, 75, 146–159.
- (1981) Omime acid rocks, Kii Peninsula—Petrogenesis. *Journal of the Japanese Association of Mineralogists, Petrologists, and Economic Geologists*, 76, 195–206.
- Lacroix, A. (1902) Note préliminaire sur une nouvelle espèce minérale. *Bulletin de la Société française de Minéralogie*, 25, 85–86.
- (1903) Sur une nouvelle espèce minérale. *Comptes Rendus Hebdomadaires des Séances de la Académie des Sciences, Paris*, 137, 582–584.
- Lacroix, A. and de Gramont, A. (1919) Sur la présence du bore dans quelques silico-aluminates basiques naturels. *Comptes Rendus Hebdomadaires des Séances de la Académie des Sciences, Paris*, 168, 857–861.
- London, D. (1992) Phosphorus in S-type magmas: The P<sub>2</sub>O<sub>5</sub> content of feldspars from peraluminous granites, pegmatites, and rhyolites. *American Mineralogist*, 77, 126–145.
- Mandarino, J.A. (1981) The Gladstone-Dale relationship: Part IV. The compatibility concept and its application. *Canadian Mineralogist*, 19, 441–450.
- (1999) *Fleischer's Glossary of Mineral Species 1999*. The Mineralogical Record Inc., Tucson, Arizona.
- McGee, J.J. and Anovitz, L.M. (1996) Electron probe microanalysis of geologic materials for boron. In L.M. Anovitz and E.S. Grew, Eds., *Boron: Mineralogy, Petrology and Geochemistry*, 33, 771–788. *Reviews in Mineralogy, Mineralogical Society of America*, Washington, D.C.
- McKie, D. (1965) The magnesium aluminium borosilicates: kornepurine and grandidierite. *Mineralogical Magazine*, 34, 346–357.
- Murata, M. (1982) S-type and I-type granitic rocks of the Ohmine district, central Kii peninsula. *Journal of the Japanese Association of Mineralogists, Petrologists, and Economic Geologists*, 77, 267–277 (in Japanese with abstract in English).
- (1984) Petrology of Miocene I-type and S-type granitic rocks in the Ohmine district, central Kii peninsula. *Journal of the Japanese Association of Mineralogists, Petrologists, and Economic Geologists*, 79, 351–369 (in Japanese with abstract in English).
- Murata, M. and Itaya, T. (1987) Sulfide and oxide minerals from S-type and I-type granitic rocks. *Geochimica et Cosmochimica Acta*, 51, 497–507.
- Murata, M. and Yoshida, T. (1985) Trace elements behavior in Miocene I-type and S-type granitic rocks in the Ohmine district, central Kii peninsula. *Journal of the Japanese Association of Mineralogists, Petrologists, and Economic Geologists*, 80, 227–245 (in Japanese with abstract in English).
- Murata, M., Itaya, T., and Ueda, Y. (1983) Sulfide and oxide minerals from the Ohmine granitic rocks in Kii Peninsula, central Japan, and their primary paragenetic relations. *Contributions to Mineralogy and Petrology*, 84, 58–65.
- Olesch, M. and Seifert, F. (1976) Synthesis, powder data and lattice constants of grandidierite, (Mg,Fe)Al<sub>3</sub>SiBO<sub>9</sub>. *Neues Jahrbuch für Mineralogie Monatshefte*, 1976, 513–518.
- Peacor, D.R., Rouse, R.C., and Grew, E.S. (1999) Crystal structure of boralsilite and its relation to a family of borosaluminosilicates, sillimanite, and andalusite. *American Mineralogist*, 84, 1152–1161.
- Pichavant, M. (1981) An experimental study of the effect of boron on a water saturated haplogranite at 1 kbar vapour pressure. *Contributions to Mineralogy and Petrology*, 76, 430–439.
- Qiu, Z.-M., Rang, M., Chang, J.-T., and Tan, M.-J. (1990) Mössbauer spectra of grandidierite. *Chinese Science Bulletin*, 35, 43–47.
- Seifert, F. and Olesch, M. (1977) Mössbauer spectroscopy of grandidierite, (Mg,Fe)Al<sub>3</sub>SiBO<sub>9</sub>. *American Mineralogist*, 62, 547–553.
- Shibata, K. (1978) Contemporaneity of Tertiary granites in the Outer Zone of Southwest Japan. *Bulletin of the Geological Survey of Japan*, 29, 551–554 (text in Japanese).
- Shiida, I., Suwa, K., Umeda, K., and Hoshino, M. (1989) Geology of the Sanjogatake district. With Geological Sheet Map at 1:50,000, Geological Survey of Japan, 100 p. (in Japanese with English abstract 5 p.).
- Stephenson, D.A. and Moore, P.B. (1968) The crystal structure of grandidierite, (Mg,Fe)Al<sub>3</sub>SiBO<sub>9</sub>. *Acta Crystallographica*, B24, 1518–1522.
- Su, S.-C. (1993) Determination of refractive index of solids by using dispersion staining method: An Analytical Approach. In G.W. Bailey and C.L. Rieder, Eds., *Proceedings of 51st Annual Meeting of the Microscopy Society of America*, p. 456–457, Chicago, U.S.A.
- Su, S.-C. (1998) Dispersion staining: Principles, analytical relationships and practical applications to the determination of refractive index. *The Microscope*, 46, 123–146.
- Su, S.-C., Bloss, F.D. and Gunter, M. (1987) Procedures and computer programs to refine the double variation method. *American Mineralogist*, 72, 1011–1013.
- Takahashi, M. (1986) Magmatic activity of island arcs just before and after the opening of the Japan Sea. *Kagaku*, 56, 103–111 (in Japanese).
- Takahashi, M., Aramaki, S., and Ishihara, S. (1980) Magnetite-series/Ilmenite-series vs. I-type/S-type granitoids. *Mining Geology Special Issue No. 8*, 13–28.
- Tan, M.-J. and Lee, H.-C. (1988) Discovery of grandidierite in China. *Geological Science and Technology Information*, 7, 30 (in Chinese).
- Terakado, Y., Shimizu, H., and Masuda, A. (1988) Nd and Sr isotopic variations in acidic rocks formed under a peculiar tectonic environment in Miocene Southwest Japan. *Contributions to Mineralogy and Petrology*, 99, 1–10.
- Tuttle, O.F. and Bowen, N.L. (1958) Origin of granite in the light of experimental studies in the system NaAlSi<sub>3</sub>O<sub>8</sub>-KAlSi<sub>3</sub>O<sub>8</sub>-SiO<sub>2</sub>-H<sub>2</sub>O. *Geological Society of America, Memoir*, 74, 153 p.
- von Knorring, O., Sahama, T.G., and Lehtinen, M. (1969) A note on grandidierite from Fort Dauphin, Madagascar. *Bulletin of the Geological Society of Finland*, 41, 71–74.
- White, A.R.J. and Chappell, B.W. (1977) Ultrametamorphism and granitoid genesis. *Tectonophysics*, 43, 7–22.

MANUSCRIPT RECEIVED FEBRUARY 26, 2001

MANUSCRIPT ACCEPTED AUGUST 21, 2001

MANUSCRIPT HANDLED BY JOHN RAKOVAN